Ligand Interaction between Urokinase-Type Plasminogen Activator and Its Receptor Probed with 8-Anilino-1-naphthalenesulfonate. Evidence for a Hydrophobic Binding Site Exposed Only on the Intact Receptor†

Michael Ploug,*,‡ Vincent Ellis,‡,§ and Keld Danø‡

Finsen Laboratory, Rigshospitalet, Strandboulevarden 49, DK-2100 Copenhagen Ø, Denmark, and Thrombosis Research Institute, Emmanuel Kaye Building, Manresa Road, London SW3 6LR, U.K.

Received March 7, 1994; Revised Manuscript Received May 16, 1994®

ABSTRACT: The cellular receptor for urokinase-type plasminogen activator (uPAR) is a glycolipid-anchored membrane protein thought to play a primary role in the generation of pericellular proteolytic activity, and to be involved in cancer cell invasion and metastasis. This protein is composed of three homologous domains, the NH_2-terminal of which is involved in the high-affinity binding ($K_d \approx 0.1$–1.0 nM) to the epidermal growth factor-like module of urokinase-type plasminogen activator (uPA). Here we report that intact uPAR binds the low molecular weight fluorophore 8-anilino-1-naphthalenesulfonate (ANS) to form a 1:1 stoichiometric complex and that the resulting enhancement of the ANS fluorescence probes the functional state of uPAR as judged by several independent criteria. First, the uPAR-mediated increase in ANS fluorescence can be titrated by uPA as well as by its receptor binding derivatives (the amino-terminal fragment and the growth factor-like module). Second, an anti-uPAR monoclonal antibody, capable of preventing uPA binding, can also titrate the uPAR-dependent ANS fluorescence whereas other antibodies not interfering with uPA binding are unable to exert this effect. Third, the dissociation profile of uPA–uPAR complexes as a function of increasing concentrations of guanidine hydrochloride closely parallels the loss of the ANS binding site in uPAR. Finally, liberation of the NH_2-terminal domain from uPAR by limited chymotrypsin cleavage after Tyr^{87} leads to a loss of both enhanced ANS fluorescence and high-affinity uPA binding. This latter effect, a 1500-fold decrease in uPA-binding affinity to isolated NH_2-terminal domain, demonstrates that this domain of uPAR does not contain all the determinants necessary for uPA binding, possibly due to a requirement for interdomain interactions to either stabilize an active conformation of this domain or be directly involved in the binding process.

In recent years it has become increasingly evident that plasminogen activation catalyzed by cell surface-associated urokinase-type plasminogen activator (uPA)[1] plays an important role in a variety of physiological as well as pathophysiological processes, including cancer cell invasion and metastasis (Ellis et al., 1992). The high-affinity binding ($K_d \approx 0.1$–1.0 nM) of uPA to cell surfaces is exclusively mediated by the uPA receptor (uPAR), which among other cells is expressed on neutrophils, monocytes, migrating keratinocytes (Vassalli et al., 1985; Ploug et al., 1992; Rømer et al., 1994), and various cancer cells and cell lines of neoplastic origin (Blasi, 1988; Pyke et al., 1991).

The cDNA for uPAR encodes a 335-residue polypeptide which after removal of the signal sequence (Roldan et al., 1990) is further truncated during the posttranslational removal of a COOH-terminal signal peptide responsible for the addition of a glycolipid membrane anchor (Ploug et al., 1991a). The mature uPAR sequence (residues 1–283) is divided into three cysteine-rich repeats of approximately 90 amino acids covering the entire sequence, and it has therefore been proposed that uPAR is composed of three homologous domains (Behrendt et al., 1991; Ploug et al., 1991b). The internal repeats of uPAR appear to be related to a family of single-domain, glycolipid-anchored membrane glycoproteins, which includes the membrane inhibitor of reactive lysis (MIRL/CD59) and the murine Ly-6 antigens (Palfree, 1991; Ploug et al., 1991b). Recently, the disulfide bond connectivity of the NH_2-terminal domain of uPAR has been solved (Ploug et al., 1993) and has been found to be homologous to that of the nonglycosylated snake venom α-neurotoxins, suggesting that the individual uPAR domains adopt the same overall structural topology as these toxins. Recent ^{1}H-NMR assignments for MIRL/CD59 are consistent with a model in which this protein, homologous to the uPAR domains, has a gross folding topology similar to that of the snake α-neurotoxins (Fletcher et al., 1993).

The interaction between uPA and uPAR is entirely governed by the high receptor-binding affinity of the small epidermal growth-factor like module of uPA: a mosaic protein which also contains a kringle module and a serine protease domain (Mazar et al., 1992). The structural elements within uPAR responsible for this high-affinity interaction appear in contrast more complex and have not yet been clarified in detail. It has, however, been shown previously that the NH_2-terminal domain of uPAR (residues 1–87) associates with uPA since, first, a covalently cross-linked adduct between this domain and uPA can be formed selectively using disuccinimidyl suberate (Behrendt et al., 1991) and, second, a monoclonal antibody reactive with this domain inhibits uPA binding to cells (Rønne et al., 1991).

† This work was supported financially by the Danish Cancer Society and the Danish Biotechnology Program.

* Correspondence should be addressed to this author at the Finsen Laboratory, Rigshospitalet Opg. 86.21, Strandboulevarden 49, DK-2100 Copenhagen Ø, Denmark. Tel: +45-35455708; FAX: +45-31385450.

‡ Finsen Laboratory, Rigshospitalet.

§ Thrombosis Research Institute.

® Abstract published in *Advance ACS Abstracts,* July 1, 1994.

[1] Abbreviations: ANS, 8-anilino-1-naphthalenesulfonic acid; ATF, amino-terminal fragment of uPA; GFD, growth factor-like domain of uPA; uPA, urokinase-type plasminogen activator; uPAR, uPA receptor.

0006-2960/94/0433-8991$04.50/0

In this paper we report that the extrinsic fluorophore 8-anilino-1-naphthalenesulfonate (ANS) binds to a single hydrophobic site exposed on intact uPAR and that the enhancement of the fluorescence of bound ANS probes the surface expression of a high-affinity binding site for uPA. In addition, we show that chymotrypsin cleavage after Tyr^{87} in uPAR greatly reduces the affinity toward uPA and that such cleavages in the linker region between domains I and II of uPAR is parallelled by a concomitant loss of ANS binding.

MATERIALS AND METHODS

Chemicals and Reagents. 8-Anilino-1-naphthalenesulfonic acid (ANS) was from Sigma (St. Louis, MO), stored as a stock solution of 100 mg/mL in water, and its molar concentration was determined spectrophotometrically using ϵ_{386} = 3985 M^{-1} cm^{-1}. Guanidine hydrochloride was of ARISTAR grade from British Drug House (Poole, U.K.). Phosphate-buffered-saline (PBS) consisted of 10 mM sodium phosphate, pH 7.4, and 0.15 M NaCl.

Purified Proteins. Recombinant pro-uPA (EC 3.4.21.31) expressed in *Escherichia coli* was a kind gift from Dr. D. Saunders (Grünenthal, Germany). The following purified uPA derivatives were kindly provided by Drs. A. Mazar and J. Henkin (Abbott, IL): the amino-terminal fragment (ATF) of uPA (residues 6–135), the epidermal growth factor-like module (GFD) of uPA (residues 4–43), the urokinase kringle (residues 47–135), and low molecular weight uPA (residues 136–411) containing the serine protease domain [for further details see Mazar et al. (1992)]. A soluble, truncated uPAR derivative (residues 1–277) was purified by immunoaffinity chromatography from the conditioned media of transfected Chinese hamster ovary cells (Ploug et al., 1993) and quantified spectrophotometrically using $E^{1\%}_{280nm}$ = 9.2 (Rønne et al., 1994). Monoclonal antibodies to human uPAR (R2, R3, and R5) were produced and characterized as described previously (Rønne et al., 1991).

Trypsin (EC 3.4.21.4) treated with *N*-tosyl-L-phenylalanine chloromethyl ketone and α-chymotrypsin (EC 3.4.21.1) were purchased from Worthington (Freehold, NJ). Human neutrophil elastase (EC 3.4.24.27) was from Calbiochem (La Jolla, CA), and thermolysin was from Daiwa Kasie (Osaka, Japan).

Generation and Purification of uPAR Domain I and Domain II + III. Purified uPAR (750 μg) was incubated with α-chymotrypsin (100 ng) for 4 h at 37 °C in 0.1 M NH_4HCO_3 before the digestion was terminated by the addition of 1 mM phenylmethanesulfonyl fluoride. Domain I was separated from the remaining intact uPAR and domain II + III by size exclusion chromatography using a Superdex 75 HR 10/30 column (Pharmacia) as described previously (Ploug et al., 1993). This preparation of uPAR domain I was acidified by addition of trifluoroacetic acid and subjected to reversed-phase chromatography on a ProRPC HR 5/2 column (Pharmacia) with a linear gradient (1 h) of 0.1% (v/v) trifluoroacetic acid in water to 70% (v/v) 2-propanol containing 0.085% (v/v) trifluoroacetic acid at a flow rate of 300 μL/min. This procedure separates uPAR domain I from small quantities of a further truncated derivative (shown as uPAR domain I′ in Figure 2A).

The fractions from the size exclusion chromatography containing uPAR domain II + III were subjected to immunoaffinity chromatography using an anti-uPAR monoclonal antibody (R3—recognizing an epitope on domain I) immobilized on *N*-hydroxysuccinimide-activated Superose HR 10/2 (Pharmacia) to remove intact uPAR and domain I. The run-through containing domain II + III was finally subjected to a second size exclusion chromatography on Superdex 75, after which the descending part of the eluted peak was collected.

Cell-Binding Experiments. The affinity of uPA for uPAR and its proteolytic derivatives was determined in an assay in which the binding of ^{125}I-labeled ATF to U937 cells was competed by various uPAR preparations. U937 cells were grown under standard conditions and washed in acidic buffer to remove endogenously bound uPA as described previously (Ellis et al., 1993). Aliquots (100 μL) of cells (1×10^7 cells/mL) were resuspended in PBS containing 0.1% bovine serum albumin prior to the addition of 10-μL aliquots of varying dilutions of the uPAR preparations followed by 10 μL of ^{125}I-labeled ATF (50 ng/mL and 2.6 μCi/mL). These were incubated for 2 h at 4 °C with shaking. Aliquots (100 μL) were then layered on to 200 μL of oil mixture (85:15, v/v, of dimethyldiphenylpolysiloxane and ρ = 0.88 g/mL mineral oil) in polypropylene microcentrifuge tubes, before centrifugation at 14000*g* for 3 min, amputation of the tube tips, and γ-radioactivity counting. Specific ATF binding isotherms were then constructed.

Fluorescence Measurements. Fluorescence emission spectra of ANS were obtained with a Perkin-Elmer LS-5 spectrofluorimeter using an excitation wavelength of 386 nm and recording emission over the range 400–600 nm, using 5-nm band-pass excitation and emission slits and 5-mm path length quartz cuvettes. When the response of the uPAR-dependent ANS fluorescence was measured as a function of a certain treatment (*e.g.*, proteolysis, titration with monoclonal antibodies or uPA derivatives) excitation was at 386 nm and emission was recorded at a fixed wavelength of 470 nm. All fluorescence measurements were made using 2 μM uPAR and 10 μM ANS in PBS at 25 °C unless otherwise stated.

ANS Titration. The stoichiometry and affinity of ANS binding to uPAR were determined by titrating fixed concentrations of uPAR with ANS up to a concentration of 100 μM. The observed fluorescence intensities were corrected for the dilution effect of the added ANS, for the low background fluorescence of ANS in buffer, and for the inner filter effect of the varying concentration of ANS. The latter was performed using the relationship $F_{corr} = F_{obs}[(2.303\epsilon_{386}[ANS]_0)/(1 - 10^{-\epsilon_{386}[ANS]_0})]$, where ϵ_{386} is the molar extinction coefficient of ANS at half the path length of the fluorescence cuvette, $[ANS]_0$ is the total ANS concentration, and F_{obs} and F_{corr} are the observed and corrected fluorescence intensities. The concentration of bound ANS was determined from the relationship $[ANS]_B = F_{corr}/F_{max}$, where F_{max} is the theoretical fluorescence of a molar solution if all were bound to uPAR. This parameter was calculated by titration of a protein concentration sufficiently high to ensure that essentially all added ANS is bound in the initial linear part of the binding curve. The data generated in this way were analyzed by the method of Scatchard.

UV Absorption Difference Spectra. The difference between the ultraviolet absorption spectra of uPAR before and after limited chymotrypsin degradation was determined using a Beckman DU-70 spectrophotometer. The UV spectrum was recorded digitally at intervals of 0.05 nm for uPAR at a concentration of 60 μM in PBS at 25 °C, prior to the addition of 1/1000 volume of a stock solution of chymotrypsin (60 μM). Additional spectra were recorded until completion of proteolysis, as judged by lack of further spectral changes. Difference spectra were generated by subtraction of the individually recorded spectra. In a control experiment,

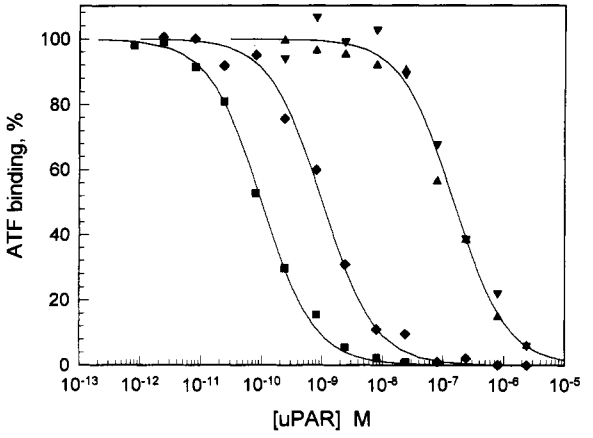

FIGURE 1: Inhibition of binding of ^{125}I-labeled ATF to U937 cells by varying amounts of intact uPAR or uPAR treated with different concentrations of chymotrypsin. U937 cells were incubated with varying concentrations of either intact uPAR (■) or uPAR treated with chymotrypsin at molar ratios of 1:10 000 (♦), 1:1000 (▲) and 1:100 (▼) as described in the legend to Figure 2. The cells were then incubated with ^{125}I-labeled ATF, and specific ATF binding was determined after subtraction of counts not competable by a large excess of intact uPAR (this nonspecific binding never exceeded 10% of the total ATF binding). Mean data from triplicate determinations are shown expressed as a percentage of ATF binding in the absence of added uPAR.

performed by substituting chymotrypsin with PMSF-treated chymotrypsin under otherwise identical conditions, no absorption difference spectrum was generated.

Miscellaneous Analyses. Detection of uPAR and its functional derivatives was performed by chemical cross-linking using *N,N'*-disuccinimidyl suberate essentially as described (Nielsen et al., 1988). SDS–PAGE of reduced and alkylated samples was according to Laemmli (1970) and was performed in a Bio-Rad Mini-Protean II apparatus.

RESULTS

Chymotrypsin Cleavage in the Linker Region of uPAR Reduces Its Affinity for uPA. We have previously demonstrated that limited chymotrypsin cleavage of uPAR liberates the NH_2-terminal domain (residues 1–87) from the remaining domain II + III due to a single cleavage after Tyr^{87} (Behrendt et al., 1991). By chemical cross-linking to ^{125}I-labeled ATF it was furthermore shown that only the NH_2-terminal domain had retained the capability to bind the ligand (Behrendt et al., 1991). The availability of larger amounts of uPAR protein in the form of recombinant soluble uPAR (residues 1–277) has allowed us to further investigate the characteristics of this binding. To determine whether the affinity of ligand binding was altered by chymotrypsin treatment, we subjected purified recombinant soluble uPAR (subsequently referred to simply as uPAR) to various chymotrypsin concentrations and subsequently tested the degradation mixture in a competitive radiolabeled ligand binding assay, in which the binding of ^{125}I-labeled ATF to U937 cells was competed by these uPAR preparations. As shown in Figure 1, intact uPAR competed with an IC_{50} of 0.1 nM, which under the experimental conditions used approximates to the K_d of the interaction between uPAR and ATF. However, with increasing chymotrypsin concentrations there was a large decrease in the affinity of the interaction, with the K_d increasing 1500-fold to 150 nM.

As revealed by SDS–PAGE and Coomassie staining (Figure 2A), the higher chymotrypsin concentrations led to a complete conversion of intact uPAR, producing uPAR domain II + III along with uPAR domain I and a further truncated derivative referred to as uPAR I' in the figure (cleavage after Tyr^{87} and Tyr^{57}, respectively). When these samples were subjected to chemical cross-linking to ^{125}I-labeled ATF (Figure 2B), they exhibited a decrease in binding activity after chymotrypsin treatment comparable to that observed in the cell binding experiment (Figure 1). Cross-linking of ATF to uPAR domain I could only be detected using a 100-fold higher concentration of uPAR (10 nM), consistent with a much reduced affinity (Figure 2C, lane 3). At these high uPAR concentrations trace amounts of residual intact protein could be detected due to the sensitivity of the method, which possibly contributed to the competitive effect of the chymotrypsin degradation mixture observed above.

In a separate experiment (data not shown), reversed-phase HPLC-purified uPAR domain I (residues 1–87) was unable to compete ATF binding to U937 cells even at concentrations as high as 1 μM, despite being able to form a specific covalent complex in cross-linking experiments with an efficiency not distinguishable from that of the degradation mixture. A purified preparation of uPAR domain II + III was able to compete the binding of ^{125}I-labeled ATF to U937 cells with a K_d of 250 nM, but it cannot be excluded that this was due to trace contamination (<0.1%) with intact uPAR, which could be detected (but not quantified) by cross-linking using high concentrations of the preparation.

UV Absorption Difference Spectrum. To investigate the basis of this very large reduction in ligand binding affinity upon proteolytic liberation of uPAR domain I, we sought spectral probes that might reflect differences between intact and partially degraded uPAR. The UV absorption difference spectrum produced by chymotrypsin treatment of uPAR is shown in Figure 3. The UV absorption spectrum of uPAR is blue shifted by this limited proteolysis due to increased solvent exposure of aromatic residues; the minima at 292 and 285 nm indicate net tryptophan exposure while the relative magnitude of the minimum at 285 nm also indicates an additional involvement of tyrosine residue exposure, as does the small minimum at 278 nm (Herskovits, 1967). It should be noted however that these changes are relatively small and would be accounted for by an approximately 30% increase in solvent exposure of single tryptophan and tyrosine residues.

uPAR Binds 8-Anilino-1-naphthalenesulfonate (ANS). Hydrophobic interactions often play an major role in protein–protein interactions, and binding of the extrinsic fluorophore ANS to such exposed hydrophobic portions of the protein can be monitored by the accompanying increase in the quantum yield of the fluorescence (Stryer, 1965). We therefore investigated the ANS binding properties of intact uPAR. As shown in Figure 4, uPAR was indeed found to bind ANS and gave a large enhancement in its fluorescence intensity (>10-fold), together with a blue shift in the emission spectrum from 515 to 470 nm, changes which are consistent with ANS binding to uPAR at hydrophobic site(s) on the protein. Further analysis of the characteristics of this binding revealed that ANS bound to a single site on uPAR (1.09 ± 0.17 mol/mol of uPAR) with a dissociation constant of 33.8 ± 3.2 μM (Figure 5). These parameters compare favorably to those of other proteins that specifically bind ANS: *e.g.*, complement component C3b binds two molecules of ANS with K_d = 40 μM (Isenman, 1983), and apohemoglobin binds one molecule of ANS per subunit with K_d = 55 μM (Stryer, 1965).

It was subsequently demonstrated (Figure 4, curve 2) that chymotrypsin cleavage of intact uPAR led to a 75% reduction in the ANS fluorescence, suggesting either that the specific

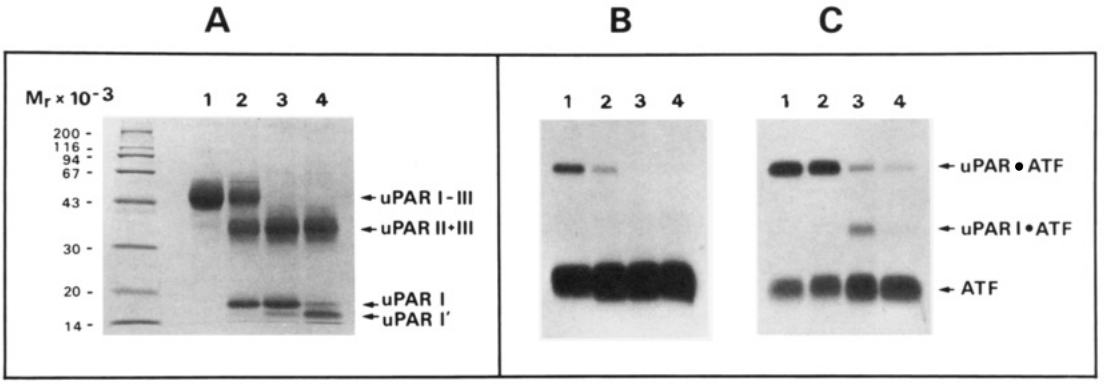

FIGURE 2: Molecular analyses of intact and chymotrypsin-treated uPAR assessed by SDS–PAGE and chemical cross-linking. Panel A shows a Coomassie-stained SDS–PAGE gel (12% T and 2.5% C) of uPAR incubated at 25 °C for 1 h either in PBS alone (lane 1) or in the presence of chymotrypsin at enzyme to substrate ratio of either 1:10 000 (lane 2), 1:1000 (lane 3), or 1:100 (lane 4). The reaction was terminated by the addition of 2 mM phenylmethanesulfonyl fluoride. Samples were reduced and alkylated, and approximately 4 μg of each was applied. The identities of the bands labeled uPAR I and uPAR I′ were revealed as residues 1–87 and 1–57, respectively, by laser desorption mass spectrometry. Panels B and C show autoradiograms of SDS–PAGE gels of samples identical to those described in panel A but subjected to a chemical cross-linking to 2 nM ^{125}I-labeled ATF at two different uPAR concentrations: 0.1 nM (panel B) and 10 nM (panel C).

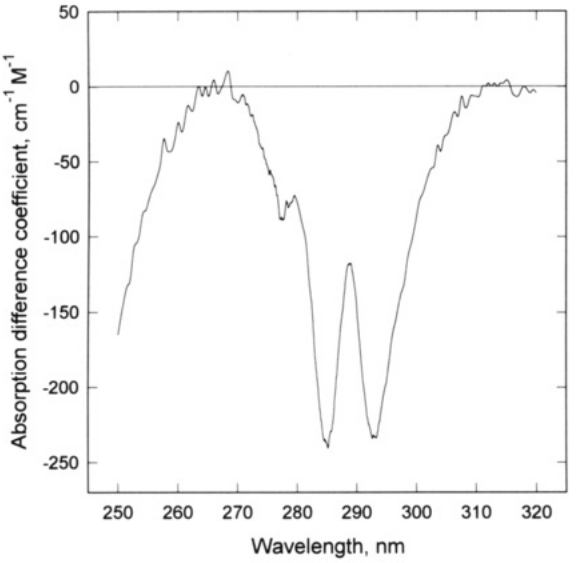

FIGURE 3: Ultraviolet absorption difference spectrum of chymotrypsin-treated versus intact uPAR. The UV difference spectrum generated on treatment of uPAR with a 1:1000 molar ratio of chymotrypsin for 30 min is shown.

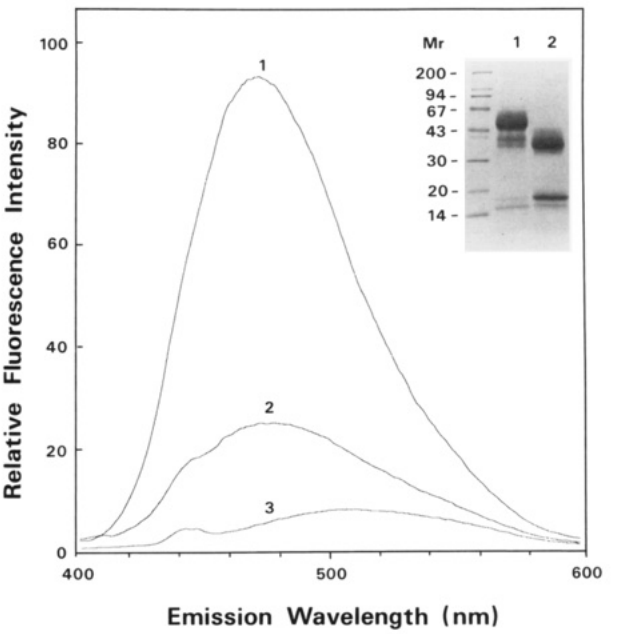

FIGURE 4: Change in the ANS fluorescence properties of uPAR following cleavage after Tyr^{87} by chymotrypsin, thereby liberating domain I from domains II + III. After recording the initial spectrum for 2 μM uPAR (curve 1), the sample was treated with 0.4 nM chymotrypsin for 3 h at 37 °C before the second spectrum of cleaved uPAR was recorded (curve 2). The buffer control is PBS with 10 μM ANS (curve 3). Inset: SDS–PAGE (12% T and 2.5% C) of 5 μg of uPAR before (lane 1) and after (lane 2) the chymotrypsin cleavage samples were reduced and alkylated. A small amount of "auto-degradation" is observed in the mock treated control sample (cleavage after Arg^{58} and Arg^{89}—as determined by laser desorption mass spectrometry).

binding site for ANS had been lost or that the microenviroment of the bound ANS became less hydrophobic, causing a lower fluorescence quantum yield. The former possibility is favored by the fact that the wavelength of the fluorescence emission maximum did not change upon chymotrypsin cleavage. Other proteases including trypsin, neutrophil elastase, thermolysin, and uPA that cleave in the linker region between domains I and II of uPAR caused a similar decrease in the ANS fluorescence intensity (data not shown).

Titration of Receptor-Bound ANS by uPA, ATF, and GFD. As both the enhanced ANS fluorescence and the high affinity for uPA were decreased on chymotrypsin cleavage of uPAR, we sought to determine whether the binding of ANS was reporting directly on the integrity of the uPA binding site of uPAR. Addition of an equimolar amount of pro-uPA to a solution of uPAR caused a reduction in ANS fluorescence equivalent to that obtained upon chymotrypsin cleavage (Figure 6). The dependence of this effect on the direct interaction between uPA and uPAR was demonstrated using smaller derivatives of uPA. Both ATF and GFD (residues 6–135 and 4–43, respectively) gave a similar reduction in fluorescence to that observed with pro-uPA (Figure 6). In contrast, neither the isolated serine protease domain nor the kringle domain (residues 136–411 and 47–135, respectively) had any effect on the ANS fluorescence when added at equimolar concentrations (data not shown). Therefore, the enhancement of ANS fluorescence on binding to uPAR reflects the availability of a functional, *i.e.*, high-affinity, uPA binding site.

Titration of Receptor-Bound ANS by Monoclonal Antibodies. To test whether macromolecular ligands other than uPA also influence the ANS binding properties of uPAR, we measured the enhanced ANS fluorescence as a function of increasing concentrations of three different anti-uPAR monoclonal antibodies. Figure 7 shows that only one of these antibodies, R3, affected the fluorescence, reducing it to a level

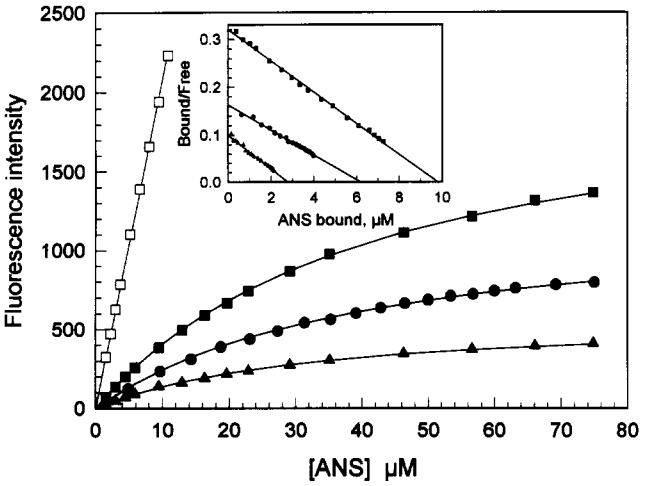

FIGURE 5: Fluorescence titration of uPAR with ANS. Titration of varying concentrations of uPAR (▲ 2.5 μM, ● 5.3 μM, ■ 10.1 μM, □ 68 μM) with ANS is shown in the main panel. The fluorescence intensities have been corrected for dilution, the background from unbound ANS, and inner filter effects as described in Materials and Methods. The inset shows a Scatchard transformation of these data, from which the stoichiometry and affinity of ANS binding were calculated.

comparable to that observed after titration with uPA. The R3 antibody has its epitope on uPAR domain I and has previously been shown to prevent the binding of uPA; consistent with this, addition of an equimolar amount of uPA to this uPAR/R3 mixture caused no further reduction in fluorescence. Therefore, this antibody mimics the effect of uPA on the interaction between ANS and uPAR. In contrast, ANS fluorescence was not affected by the presence of R2 (recognizing an epitope on domain II + III). Subsequent addition of uPA reduced the fluorescence to a level equivalent to that obtained in the absence of the antibody. Addition of the third antibody, R5, recognizing an epitope on domain I distinct from that of R3, and that does not block the cellular binding of uPA (E. Rønne, unpublished data), also had no effect on ANS fluorescence. With this antibody addition of uPA caused a reduction in the ANS fluorescence approximately 50% of that observed in the presence of R2, possibly due to a minor steric hinderance of uPA binding in the presence of R5.

Denaturant-Induced Loss of ANS and Pro-uPA Binding Sites on uPAR. Exposure of uPAR to increasing concentrations of guanidine hydrochloride caused a decrease in both the ANS fluorescence and uPA–uPAR complex formation with almost superimposable transition curves having midpoints at 0.8 M guanidine hydrochloride (Figure 8). No change in the wavelength of the ANS fluorescence emission maximum was observed during the guanidine-induced unfolding, suggesting that the observed changes in the ANS fluorescence intensity at 470 nm reflect an equilibrium between molecules which have retained the native structure and those which have lost their ability to bind ANS. A similar equilibrium also exists between monomers and bimolecular uPA–uPAR complexes determined by size exclusion chromatography. Addition of equimolar amounts of pro-uPA to these samples reduced the ANS fluorescence to the same end level irrespective of the concentration of guanidine hydrochloride.

The unfolding of the ANS and uPA binding sites of uPAR occurs at rather low guanidine concentrations (*i.e.*, predenaturational conditions) compared to the transition of the intrinsic tryptophan fluorescence which had its midpoint at 2 M guanidine hydrochloride (data not shown).

DISCUSSION

We have studied the interaction between uPA and its specific cellular receptor using a recombinant secreted variant of uPAR (residues 1–277) which is lacking the carboxyl-terminal signal sequence for GPI anchorage, expressed in CHO cells (Ploug et al., 1993). This variant is shown to have uPA binding characteristics equivalent to those of both the membrane-bound (Blasi, 1988) and purified wild-type protein (Ellis et al., 1993), as determined by its affinity for uPA in a competitive ligand binding assay. Using this recombinant protein, we have now established that the low molecular weight fluorophore ANS can be used as an extrinsic probe that reports on the availability of the high-affinity binding site for uPA. ANS binds to a single site on uPAR with relatively high affinity. This binding leads to a large increase and blue shift in the fluorescence emission spectrum, properties that are consistent with an interaction at a hydrophobic site on the protein. The binding of ANS correlates to the high-affinity binding of uPA as judged by the following criteria: (i) the growth factor-like module of uPA abolishes the enhanced fluorescence of ANS on binding to uPAR, (ii) a monoclonal antibody inhibiting uPA binding to uPAR also abolishes the enhanced ANS fluorescence, (iii) on partial unfolding of uPAR with guanidine hydrochloride the binding of ANS and complex formation with uPA are reduced in parallel, and (iv) proteolytic liberation of domain I leads to a loss of both high-affinity uPA binding and enhanced ANS fluorescence.

The large decrease in uPA binding affinity (at least 1500-fold) after proteolytic liberation of uPAR domain I was rather unexpected, since the specificity of chemical cross-linking to uPA has previously been shown to be retained in isolated domain I (Behrendt et al., 1991). This can be contrasted to the case with uPA, in which the small receptor-binding domain (*i.e.*, the growth factor-like module) retains full binding affinity when isolated from the rest of the protein (Mazar et al., 1992). The recently solved solution structure of the entire NH_2-terminal fragment of uPA (*i.e.*, the growth factor-like module and the kringle module) provides an explanation for this as these two domains were shown to be structurally independent with no interdomain interactions (Hansen et al., 1994). Although uPAR loses high affinity for uPA after cleavage in the "linker" region between domains I and II, structural data nevertheless suggest that a three-domain model for uPAR is valid. uPAR belongs to the Ly-6 protein family, the other members of which are single-domain glycolipid-anchored proteins and are homologous to each of the three putative domains of uPAR. Further evidence for the structural independence of the individual domains of uPAR comes from recent data suggesting that these domains are also homologous to snake venom α-neurotoxins, which are secreted single-domain proteins (Flemming et al., 1993). The structural basis for the lack of high-affinity uPA binding to uPAR domain I is therefore not apparent; however, two alternative hypotheses can be proposed.

First, proteolysis could be directly destroying a site involved in uPA binding. This seems unlikely however for a variety of reasons. The proteolytic cleavage site after Tyr^{87} was still fully accessible to chymotrypsin when uPAR was in complex with uPA, which would not be expected if this region of the protein were intimately involved in the interaction with uPA. The extreme sensitivity of this site to proteolysis suggests that the interdomain sequence is a true linker region. Also, a synthetic peptide spanning this region (Asn^{77}–Glu^{94}) did not affect uPA binding to uPAR or give a direct enhancement of ANS fluorescence (M. Ploug, unpublished data).

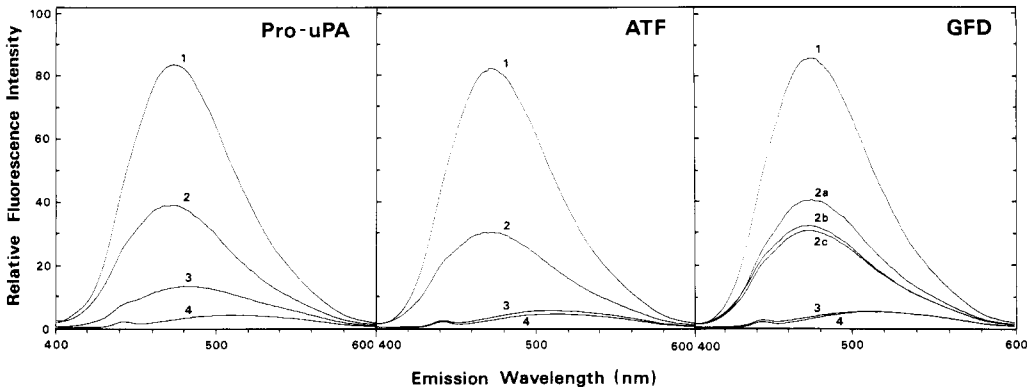

FIGURE 6: Interaction between uPA and uPAR monitored by ANS fluorescence. The emission spectra of ANS were recorded with 2 μM uPAR either alone (curve 1) or in the presence of 2 μM pro-uPA, ATF, or GFD (curve 2) as well as of 4 μM GFD (curve 2b) and 8 μM GFD (curve 2c). Also shown are the spectra for 2 μM concentrations of either ligand alone (curve 3) and a buffer control (curve 4). The volumes of added ligand never exceeded 10 μL (2.5% of the total volume).

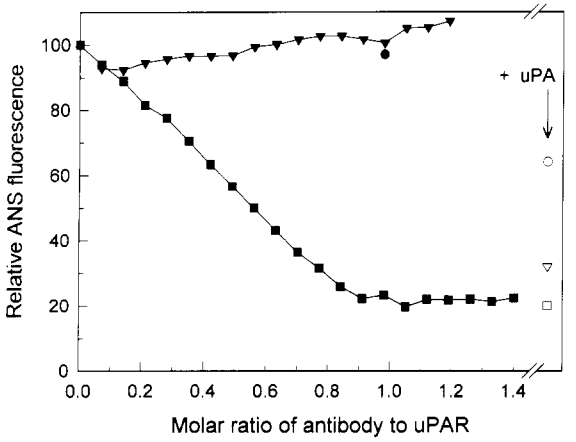

FIGURE 7: Titration of the uPAR-dependent ANS fluorescence by monoclonal antibodies. ANS fluorescence was measured for 2 μM uPAR containing increasing concentrations of three different monoclonal antibodies R2 (▼), R3 (■), and R5 (●) with excitation and emission wavelengths set at 386 and 470 nm, respectively. At the highest concentration of antibody 2 μM pro-uPA was added (shown as the respective open symbols). The ANS profiles shown have been corrected for buffer dilution as well as contribution from intrinsic fluorescence of the individual monoclonal antibodies.

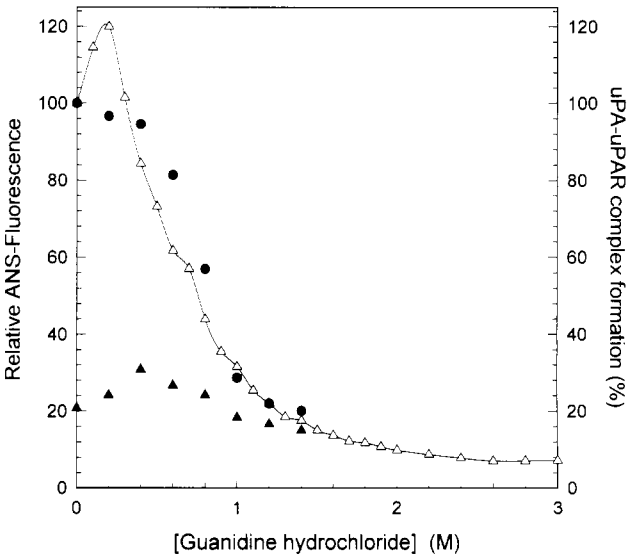

FIGURE 8: Guanidine hydrochloride interferes with binding of ANS and pro-uPA to uPAR. ANS fluorescence emission was monitored at 470 nm (excitation at 386 nm) in the presence of 2 μM uPAR containing increasing concentrations of guanidine hydrochloride dissolved in 50 mM Tris, pH 7.5, and 0.1 M NaCl (△—△). After addition of 2 μM pro-uPA the fluorescence was measured again (▲) before the samples were subjected to HPLC gel exclusion chromatography using a Superdex 200 HR10/30 column (Pharmacia) operated at 500 μL/min with the respective guanidine hydrochloride solutions. The fraction of pro-uPA and uPAR participating in bimolecular complex formation was calculated from the peak heights corresponding to monomeric and dimeric molecules (●). As monomeric uPA and uPAR have almost identical hydrodynamic volumes, they coelute during the gel filtration analysis.

Second, proteolysis could be disrupting domain–domain interactions essential for the high-affinity binding, either directly by generating a multidomain binding site for uPA or indirectly by stabilizing an "active" conformation of domain I. Association between uPAR-like domains has been demonstrated in some of the structurally homologous single-domain snake venom α-neurotoxins, in which relatively stable dimers are formed by specific interactions that generate a 6-stranded antiparallel β-sheet (Rees et al., 1990; Betzel et al., 1991; Oswald et al., 1991). For a subgroup of these toxins, exemplified by κ-bungarotoxin, it has been proposed that the dimer is the physiologically active form of the protein (Chiappinelli, 1991). We have previously observed an interaction between domain I and the remainder of the protein during size exclusion chromatography of chymotrypsin-treated uPAR (Ploug et al., 1993). However, such an interaction does not occur when isolated domain I is reconstituted with isolated domain II + III (M. Ploug, unpublished data), possibly suggesting that a conformational change occurs in one or both of the fragments subsequent to their dissociation. This is consistent with the UV difference spectrum generated on chymotrypsin cleavage of uPAR, showing changes in the local environment of the aromatic residues. The sensitivity of uPAR ligand binding to low concentrations of guanidine hydrochloride also suggests a certain lability of an active conformation of the intact protein, again potentially due to disruption of interdomain interactions.

It is notable that the putative conformational change(s) in uPAR induced by proteolytic liberation of domain I or by low concentrations of guanidine hydrochloride similarly affect the binding of both the protein ligand uPA and the low molecular weight ligand ANS. A similar equivalence in the binding of ANS and protein ligands has been observed for the interaction between human complement component C3 and its protein ligands, factors B and H. Native C3 binds neither protein ligands nor ANS, but activation by means of thioester hydrolysis (where no peptide bonds are cleaved) or proteolytic cleavage after Arg^{77} (by the physiologic C3-convertase or mimicked by trypsin) exposes binding sites for factors B and

H as well as for ANS after a conformational rearrangement in C3 (Isenman et al., 1981). Similar to the features described here for the uPA/uPAR system, the protein ligands for C3 are also able to titrate the enhanced ANS fluorescence (Isenman, 1983). In addition, further proteolytic cleavage by the physiological inactivator factor I leads to a simultaneous loss of both ANS and factor B and H binding (Isenman, 1983).

Although the proposed conformational change(s) in uPAR associated with loss of ANS and high-affinity uPA binding could potentially be occurring in any of the three domains, it seems most plausible that the structure of domain I is affected. The direct involvement of this domain in ligand binding to intact uPAR is evident from both its ability to be chemical cross-linked to uPA and the inhibition of uPA and ANS binding by the monoclonal antibody R3 which has its epitope on this domain. Among the members of the Ly-6/α-neurotoxin families uPAR domain I is unique in lacking an otherwise strictly conserved pair of cysteine residues. In all other domains these residues form one of four disulfide bridges within the small globular core of the structure determined for the α-neurotoxins, and all are thought to be involved in maintenance of the structure. The lack of this apparently essential disulfide bridge may be responsible for an inability of uPAR domain I to retain its active conformation upon dissociation from the rest of the protein. In relation to this uPAR itself is also unique among the Ly-6/α-neurotoxin proteins in having three, rather than a single, domain. It could be speculated that these two properties of uPAR, *i.e.*, the lack of a conserved disulfide bridge and its multidomain nature, are related and that the additional domains of uPAR have a role in stabilizing an otherwise labile NH_2-terminal domain.

ACKNOWLEDGMENT

We thank Dr. U. Weidle (Boehringer Mannheim, Germany) for the construction of the transfected CHO cells secreting the truncated uPAR; Drs. A. Mazar and J. Henkin (Abbott Laboratories, IL) for the purified uPA derivatives; Dr. D. Saunders (Grünenthal, Germany) for recombinant pro-uPA; and Dr. H. Rahbek-Nielsen (Odense University, Denmark) for performing the matrix-assisted laser desorption mass spectrometry. Pernille Hansen, Helle Hymøller Hald, and Bente Johannesen are thanked for excellent technical assistance.

REFERENCES

Behrendt, N., Ploug, M., Patthy, L., Houen, G., Blasi, F., & Danø, K. (1991) *J. Biol. Chem. 266*, 7842–7847.

Blasi, F. (1988) *Fibrinolysis 2*, 73–84.

Ellis, V., Pyke, C., Eriksen, J., Solberg, H., & Danø, K. (1992) *Ann. N.Y. Acad. Sci. 667*, 13–31.

Flemming, T. J., O'hUigen, C., & Malek, T. R. (1993) *J. Immunol. 150*, 5379–5390.

Fletcher, C. M., Harrison, R. A., Lachmann, P. J., & Neuhaus, D. (1993) *Protein Sci. 2*, 2015–2027.

Hansen, A. P., Petros, A. M., Meadows, R. P., Nettesheim, D. G., Mazar, A. P., Olejniczak, E. T., Xu, R. X., Pederson, T. M., Henkin, J., & Fesik, S. W. (1994) *Biochemistry 33*, 4847–4864.

Herskovits, T. T. (1967) *Methods Enzymol. 11*, 748–775.

Isenman, D. E. (1983) *J. Biol. Chem. 258*, 4238–4244.

Isenman, D. E., Kells, D. I. C., Cooper, N. R., Müller-Eberhard, H. J., & Pangburn, M. K. (1981) *Biochemistry 20*, 4458–4467.

Laemmli, U. K. (1970) *Nature 227*, 680–685.

Mazar, A. P., Buko, A., Petros, A. M., Barnathan, E. S., & Henkin, J. (1992) *Fibrinolysis 6* (Suppl. 1), 49–55.

Nielsen, L. S., Kellerman, G. M., Behrendt, N., Picone, R., Danø, K., & Blasi, F. (1988) *J. Biol. Chem. 263*, 2358–2363.

Palfree, R. G. E. (1991) *Immunol. Today 12*, 170–171.

Ploug, M., Rønne, E., Behrendt, N., Jensen, A., Blasi, F., & Danø, K. (1991a) *J. Biol. Chem. 266*, 1926–1936.

Ploug, M., Behrendt, N., Løber, D., & Danø, K. (1991b) *Semin. Thromb. Hemostasis 17*, 183–193.

Ploug, M., Plesner, T., Rønne, E., Ellis, V., Høyer-Hansen, G., Hansen, N. E., & Danø, K. (1992) *Blood 79*, 1447–1455.

Ploug, M., Kjalke, M., Rønne, E., Weidle, U., Høyer-Hansen, G., & Danø, K. (1993) *J. Biol. Chem. 268*, 17539–17546.

Pyke, C., Kristensen, P., Ralfkiær, E., Grøndhal-Hansen, J., Eriksen, J., Blasi, F., & Danø, K. (1991) *Am. J. Pathol. 138*, 1059–1067.

Roldan, A. L., Cubellis, M. V., Mascucci, M. T., Behrendt, N., Lund, L. R., Danø, K., Appella, E., & Blasi, F. (1990) *EMBO J. 9*, 467–474.

Rømer, J., Lund, L. R., Eriksen, J., Pyke, C., Kristensen, P., & Danø, K. (1994) *J. Invest. Dermatol. 102*, 519–522.

Rønne, E., Behrendt, N., Ellis, V., Ploug, M., Danø, K., & Høyer-Hansen, G. (1991) *FEBS Lett. 288*, 233–236.

Rønne, E., Behrendt, N., Ploug, M., Nielsen, H. J., Wöllisch, E., Weidle, U., Danø, K., & Høyer-Hansen, G. (1994) *J. Immunol. Methods 167*, 91–101.

Stryer, L. (1965) *J. Mol. Biol. 13*, 482–495.

Vassalli, J.-D., Baccino, D., & Belin, D. (1985) *J. Cell Biol. 100*, 86–92.